Received: 2 April 2023 | Revised: 25 May 2023 | Accepted: 30 May 2023

DOI: 10.1002/ijc.34647

IJC INTERNATIONAL JOURNAL of CANCER

RESEARCH ARTICLE

Cancer Therapy and Prevention

China special issue on gastrointestinal tumors-Radiological features of pathological complete response in mismatch repair deficient colorectal cancer after neoadjuvant PD-1 blockade: A post hoc analysis of the PICC phase II trial

Wuteng Cao[1,2,3] | Huabin Hu[2,3,4] | Jiao Li[1,2,3] | Qianyu Wu[1,2,3] | Lishuo Shi[2,3,5] | Biao Li[1,2,3] | Jie Zhou[1,2,3] | Xinhua Wang[1,2,3] | Junhong Chen[6] | Chao Wang[2,3,7] | Huaiming Wang[2,3,8] | Weihao Deng[2,3,7] | Yan Huang[2,3,7] | Yanhong Deng[2,3,4]

[1]Department of Radiology, The Sixth Affiliated Hospital, Sun Yat-sen University, Guangzhou, Guangdong, China

[2]Guangdong Provincial Key Laboratory of Colorectal and Pelvic Floor Diseases, The Sixth Affiliated Hospital, Sun Yat-sen University, Guangzhou, Guangdong, China

[3]Biomedical Innovation Center, The Sixth Affiliated Hospital, Sun Yat-sen University, Guangzhou, Guangdong, China

[4]Department of Medical Oncology, The Sixth Affiliated Hospital, Sun Yat-sen University, Guangzhou, Guangdong, China

[5]Clinical Research Center, The Sixth Affiliated Hospital, Sun Yat-sen University, Guangzhou, Guangdong, China

[6]School of Public Health (Shenzhen), Shenzhen Campus of Sun Yat-sen University, Shenzhen, Guangdong, China

[7]Department of Pathology, The Sixth Affiliated Hospital, Sun Yat-sen University, Guangzhou, Guangdong, China

[8]Department of Colorectal Surgery, Department of General Surgery, The Sixth Affiliated Hospital, Sun Yat-sen University, Guangzhou, Guangdong, China

Correspondence
Yanhong Deng, Department of Medical Oncology, The Sixth Affiliated Hospital, Sun Yat-sen University, Guangzhou, Guangdong 510655, China.
Email: dengyanh@mail.sysu.edu.cn

Funding information
National Natural Science Foundation of China, Grant/Award Numbers: 82001765, 82272800

[Correction added after first online publication on 19 July 2023. Graphical abstract, figure 3 and table 1 are updated]

Abstract

Neoadjuvant programmed cell death protein 1 (PD-1) blockade exhibits promising efficacy in patients with mismatch repair deficient (dMMR) colorectal cancer (CRC). However, discrepancies between radiological and histological findings have been reported in the PICC phase II trial (NCT 03926338). Therefore, we strived to discern radiological features associated with pathological complete response (pCR) based on computed tomography (CT) images. Data were obtained from the PICC trial that included 36 tumors from 34 locally advanced dMMR CRC patients, who received neoadjuvant PD-1 blockade for 3 months. Among the 36 tumors, 28 (77.8%) tumors achieved pCR. There were no statistically significant differences in tumor longitudinal diameter, the percentage change in tumor longitudinal diameter from baseline, primary tumor sidedness, clinical stage, extramural venous invasion status, intratumoral calcification, peritumoral fat infiltration, intestinal fistula and tumor necrosis between the pCR and non-pCR tumors. Otherwise, tumors with pCR had smaller posttreatment tumor maximum thickness (median: 10 mm vs 13 mm, $P = .004$) and higher percentage decrease in tumor maximum thickness from

Abbreviations: CI, confidence interval; CRC, colorectal cancer; CT, computed tomography; dMMR, mismatch repair deficient; EMVI, extramural venous invasion; ICC, intraclass correlation coefficient; MPR, multiplanar reformation; MRI, magnetic resonance imaging; MSI-H, microsatellite instability-high; OR, odds ratio; pCR, pathological complete response; PCR, polymerase chain reaction; PD-1, programmed cell death protein 1; RECIST, Response Evaluation Criteria in Solid Tumors; ROC, receiver operating characteristic.

Wuteng Cao, Huabin Hu, Jiao Li, Qianyu Wu and Lishuo Shi contributed equally to this study.

baseline (52.9% vs 21.6%, $P = .005$) compared to non-pCR tumors. Additionally, a higher proportion of the absence of vascular sign ($P = .003$, odds ratio [OR] = 25.870 [95% CI, 1.357-493.110]), nodular sign ($P < .001$, OR = 189.000 [95% CI, 10.464-3413.803]) and extramural enhancement sign ($P = .003$, OR = 21.667 [2.848-164.830]) was observed in tumors with pCR. In conclusion, these CT-defined radiological features may have the potential to serve as valuable tools for clinicians in identifying patients who have achieved pCR after neoadjuvant PD-1 blockade, particularly in individuals who are willing to adopt a watch-and-wait strategy.

KEYWORDS

colorectal cancer, computed tomography, neoadjuvant PD-1 blockade, pathological complete response

What's new?

While neoadjuvant PD-1 blockade exhibits promising efficacy in patients with mismatch repair-deficient colorectal cancer, discrepancies between radiological findings and pathological findings have been reported in the PICC trial. This post hoc analysis of the PICC phase II trial found that posttreatment tumor maximum thickness and the percentage change in tumor maximum thickness from baseline, as well as the absence of vascular, nodular and extramural enhancement signs were associated with pathological complete response. These easily identifiable radiological features may help clinicians and radiologists identify patients who have achieved pCR after neoadjuvant PD-1 blockade, particularly in individuals who are willing to adopt a watch-and-wait strategy.

1 | INTRODUCTION

Neoadjuvant programmed cell death protein 1 (PD-1) blockade has been heralded as a breakthrough in cancer therapy in recent years, demonstrating promising outcomes in diverse malignancies such as gastroesophageal cancer, hepatocellular carcinoma, lung cancer, breast cancer and so on.[1,2] Similarly, colorectal cancer (CRC) patients with microsatellite instability-high (MSI-H) or mismatch repair deficient (dMMR) exhibit a higher burden of mutations and are typically more responsive to neoadjuvant PD-1 blockade.[3] For resectable non-metastatic patients, the NICHE and PICC trials have revealed encouraging outcomes, with reported high rates of pathological complete response (pCR) ranging from 60% to 88%.[4,5] The promising results hold significant implications for organ preservation, particularly in rectal cancer patients.[6] In addition, the tendency of watch-and-wait strategy is gradually becoming an appropriate tactic for patients with pCR, as it allows for close monitoring and follow-up care to ensure their long-term recovery in clinical practice.[7]

Neoadjuvant chemoradiotherapy is widely employed for the management of locally advanced rectal cancer patients, aiming to decrease tumor size and facilitate surgical resection, thereby improving the likelihood of achieving complete resection and reducing the risk of disease recurrence. However, despite the radiological response in tumor regression is in line with pathological outcomes, the rate of pCR remains relatively low at approximately 20%.[8] With the advent of neoadjuvant PD-1 blockade, a new avenue for potentially increasing the pCR rate might have emerged. Nonetheless, it is noted that the assessment of tumor status via medical images may not always align with the actual pathological therapeutic effects in clinical practice, as demonstrated in the PICC trial.[5] The discrepancies might be attributed to novel response patterns, distinct from those observed with chemotherapy and chemoradiotherapy, such as pseudoprogression or hyperprogression (delayed response), leading to an increase in initial tumor size due to the immune cell infiltration.[9,10] Previous studies have indicated that some patients may derive clinical benefit from PD-1 blockade even without substantial radiological tumor shrinkage owing to this response pattern, as has been observed in dMMR advanced CRC, resected melanomas and nonsmall cell lung cancer tumors.[11-13] Such circumstances hinder the accurate assessment of therapeutic response to PD-1 blockade and informed decisions regarding individualized treatment approaches. Therefore, it is imperative to explore radiological features to accurately evaluate the therapeutic efficacy.

Computed tomography (CT) is a widely utilized procedure for the diagnosis and posttherapeutic evaluation of CRC due to its universality and noninvasive nature. Previous studies focusing on evaluating tumor response predominantly relied on the measurement of the longest tumor diameter, which should lend themselves to reproducible measurements, according to the Response Evaluation Criteria in Solid Tumors (RECIST).[11] Nonetheless, when it comes to colorectal cancer, the reassessment of target lesions could be challenging, particularly for those with poor reproducibility due to the influence of intestinal peristalsis and insufficient bowel filling. Consequently, the existing evaluation methods are still insufficient to provide a reliable reference for guiding clinical management.

In light of the substantial likelihood of pCR observed in patients with dMMR colorectal cancer following neoadjuvant PD-1 blockade,

we conducted a comprehensive analysis of CT images and investigated the pCR-related radiological features in the PICC trial.

2 | MATERIALS AND METHODS

2.1 | Patients

All 34 patients who participated in the PICC trial (NCT 03926338) were enrolled in our study. Full details regarding the PICC trial, such as inclusion and exclusion criteria, treatment schedules, ethics committee approval and main findings, have been previously reported.[5] All patients underwent enhanced thoraco-abdominopelvic CT examinations after neoadjuvant PD-1 blockade. Noted that two patients had simultaneous double primary cancers of colon and rectum and all primary tumor lesions were recorded for further analysis.

2.2 | CT imaging protocol

CT examinations were executed using the OPTIMA CT660 (GE Medical Systems, Milwaukee, Wisconsin) scanner or the AQUILION ONE (TOSHIBA Medical Systems, Japan) scanner. The scanning parameters were as follows: tube voltage, 120 kVp; tube current, 150 to 200 mA; pitch, 0.969. The nonionic contrast media iohexol (Omnipaque 300, GE Medical Systems, Chicago, Illinois) at a dose of 1.2 mL/kg weight was injected with a power injector at a rate of 2.5 mL/s through the median cubital vein, followed by 20 mL saline flushing at a rate of 3.0 mL/s. Arterial phase CT images were acquired 25 to 30 seconds after the intravenous bolus injection of the contrast agent; and the portal venous phase CT images were obtained 55 to 60 seconds after the injection. Contrast-enhanced CT was reconstructed with a reconstruction thickness of 1- or 1.25-mm thickness.

2.3 | Evaluation of CT features

All CT images were retrieved from the picture archiving and communication system for further analysis. Two radiologists (reader 1 and reader 2, with 3 and 10 years of experience, respectively), blinded to clinical-pathological information, measured the maximum thickness and the longitudinal diameter of the primary tumor as the tumor size in the pretherapeutic and posttherapeutic CT images. The multiplanar reformation (MPR) technique was applied to reconstruct the actual axial plane of tumor lesion and then measured the wall thickness in the largest cross-section area as the tumor maximum thickness. Similarly, we used the curves to measure the tumor longitudinal diameter along the longitudinal axis of the lesion based on MPR. The representative cases of tumor size measurement are shown in Supplemental Material S1.

Furthermore, we also performed a thorough analysis of the posttherapeutic CT images for each lesion, documenting the related information about the extramural venous invasion (EMVI) status, intratumoral calcification, peritumoral fat infiltration, intestinal fistula and tumor necrosis. These radiological parameters were then classified into two categories—present/positive or absent/negative. Noted that any necrosis within residual lesions in the primary tumor site appeared as an irregular low attenuation region with the CT attenuation ≤20 HU in each phase and degree of enhancement ≤10 HU.

2.4 | Novel image features derived from the posttherapeutic CT-enhanced arterial phase images

Pretherapeutic CT images were used to locate the tumor to accurately determine the extent of the lesion. CT images of arterial phase after PD-1 blockade were analyzed, including striated or punctate vessels remaining within the radiological residual tumor (vascular sign), avid enhanced mural nodules (nodular sign) in the colorectal canal invaded by the primary tumor and extramural area of colorectum with enhancement (extramural enhancement sign; Figure 1). Noted that the area outside the expected position of the normal intestinal wall was regarded as the extramural area. In the assessment of nodular and extramural enhancement signs, at least mild enhancement in extramural region was defined as a positive extramural enhancement sign, and mural nodules with avid enhancement were regarded as positive nodular sign (degree of enhancement = arterial phase CT value − plain scan CT value, 0 to 10 HU for no enhancement, 10 to 20 HU for mild enhancement, 20 to 40 HU for moderate enhancement and >40 HU for avid enhancement).[14,15] The two radiologists (reader 3 and reader 4, with 5 and 10 years of experience, respectively) were trained to assess the above three signs separately, which were dichotomized as present or absent. Should there be any divergence between the two readers, then another radiologist (reader 5, with 20 years of experience) would step in to reach a consensus or obey the majoritarian. The representative CT images of the above three signs are detailed in Supporting Information S2. Thereafter, reader 3 reassessed the signs after 2 months to assess the intra-observer agreement.

2.5 | Clinical-pathological analysis

Clinical data, including patient age at cancer diagnosis, gender, primary tumor sidedness, baseline and posttreatment staging of the primary tumor and regional lymph nodes, were collected and some had been reported in the PICC trial.[5]

All resected samples were formalin-fixed and dissected in standard histopathological analysis. The macroscopically identifiable tumor bed was dissected into serial 5- to 10-mm transverse slices, then the slices were divided into multiple blocks that were embedded and processed for hematoxylin and eosin staining in 5-μm sections. The resected samples were evaluated by experienced gastrointestinal pathologists from our institution, who were blinded to the CT data in our study. In addition, pathological T and N stages were evaluated according to the American Joint Committee on Cancer.[16]

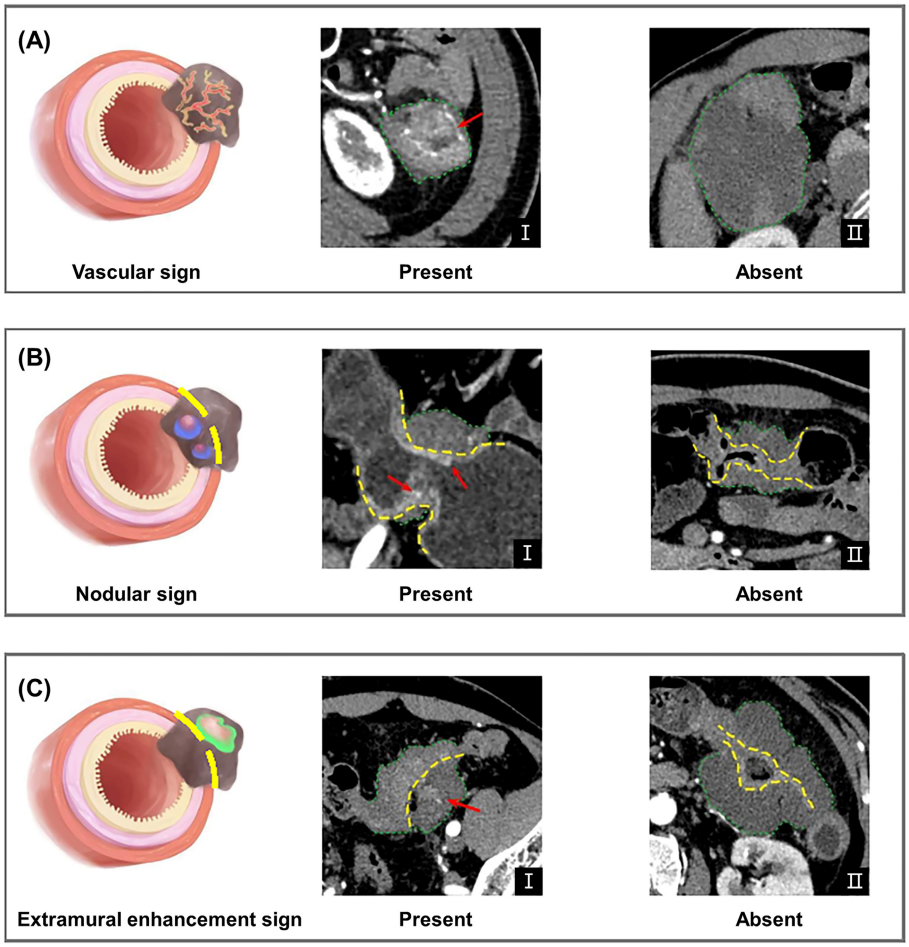

FIGURE 1 Schematic representation of vascular, nodular and extramural enhancement signs. (A) Vascular sign defined as striated or punctate vessels within the radiological residual tumor (red); the presence and absence of vascular sign are depicted in I (red arrow) and II, respectively. (B) Nodular sign meant avid enhanced mural nodules exist in the colorectal canal invaded by the primary tumor (blue); the presence and absence of nodular sign are exhibited in I (red arrow) and II, respectively. (C) Extramural enhancement sign defined as the area outside the expected normal intestinal wall with enhancement (green); the I (red arrow) and II show the presence and absence of extramural enhancement sign, respectively. The above I and II are the posttherapeutic CT arterial-phase images (the green dotted line represents the residual tumor area, and the yellow dotted line delineates the expected normal intestinal wall). Noted that the absence of the above signs is predictive for good pathological response [Color figure can be viewed at wileyonlinelibrary.com]

2.6 | Statistical analysis

The interobserver agreements between reader 1 and reader 2 for the maximum thickness and longitudinal diameter of the primary tumor were evaluated by calculating the intraclass correlation coefficient (ICC). For other CT image features, intra- or inter-reader conformance was assessed by using Kappa statistics by quantifying the Kappa (κ) coefficient. Five levels of kappa values were defined as follows: very poor reliability (κ < 0.20), poor reliability (0.21-0.40), fair reliability (0.41-0.60), moderate reliability (0.61-0.80) and good reliability (0.81-1).

All statistical analyses were conducted on a per-lesion basis, employing appropriate statistical methodologies based on the nature of the variable. The comparisons of CT imaging features characteristics between the tumors with pCR and non-pCR were performed utilizing the Chi-square test or Fisher's exact test (primary tumor sidedness, baseline and posttreatment staging of primary tumor and lymph node, EMVI status, intratumoral calcification, peritumoral fat infiltration, intestinal fistula, tumor necrosis, vascular, nodular and extramural enhancement signs). We analyzed other radiological parameters, such as the tumor maximum thickness and tumor longitudinal diameter on the pretreatment and posttreatment images, as well as their corresponding percentage changes from baseline, using either Student's T test or Mann-Whitney *U* test on a case-by-case basis. If significant statistical significance was observed in continuous data, then receiver operating characteristic (ROC) curve analysis would be performed to determine the optimal classification threshold along with the corresponding Youden index (maximizing the difference between sensitivity and specificity) in order to convert continuous data into binary data for the calculation of odds ratio (OR). Notably, the determination of final cutoff values should consider simplicity of clinical practice. For all variables demonstrating statistically significant differences, we calculated OR values and reported the 95% confidence intervals (CI) to reflect the strength of their associations with pCR.

Statistical analyses were performed by using SPSS (version 25.0 IBM, NY) and MedCalc software (version 18.2 Belgium). Statistical significance was considered when the *P* value was less than .05. GraphPad Prism 8 software was employed to visualize the distribution of CT image features.

3 | RESULTS

3.1 | Clinical characteristics

All posttherapeutic CT examinations were performed within a month after the end of the treatment and all patients in the PICC trial underwent surgical resection with R0. A total of 36 primary tumors from 34 patients were included in our study. Among these patients, four (11.8%) had rectal cancer, 28 (82.4%) had colon cancer and the remaining two (5.9%) had primary

TABLE 1 Characteristics of colorectal tumors in CT images

Variable	pCR[a] (n = 28)	Non-pCR (n = 8)	*P*-value
Primary tumor sidedness			.323
Left-sided colon	7 (25.0)	0	
Right-sided colon	17 (60.7)	6 (75.0)	
Rectum	4 (14.3)	2 (25.0)	
Tumor size			
Pretreatment tumor longitudinal diameter (mm), median (IQR)	66.5 (46.0, 79.5)	67.0 (53.0, 79.5)	.952
Posttreatment tumor longitudinal diameter (mm), median (IQR)	26.0 (16.5, 39.5)	31.5 (25.0, 48.0)	.356
Percentage change in tumor longitudinal diameter from baseline (%), median (IQR)	52.6 (38.7, 67.6)	49.2 (29.8, 61.7)	.297
Pretreatment tumor maximum thickness (mm), median (IQR)	25.0 (17.0, 29.5)	21.0 (16.5, 24.0)	.493
Posttreatment tumor maximum thickness (mm), median (IQR)	10.0 (8.0, 11.5)	13.0 (12.5, 17.5)	.004
Percentage change in tumor maximum thickness from baseline (%), median (IQR)	52.9 (37.3, 63.3)	21.6 (14.2, 36.4)	.005
Pretreatment T stage			1.000
T3	5 (17.9)	1 (12.5)	
T4a	10 (35.7)	3 (37.5)	
T4b	13 (46.4)	4 (50.0)	
Posttreatment T stage			1.000
T1-3	9 (32.1)	3 (37.5)	
T4a	10 (35.7)	3 (37.5)	
T4b	9 (32.1)	2 (25.0)	
Pretreatment N stage			1.000
N0	3 (10.7)	1 (12.5)	
N1	6 (21.4)	1 (12.5)	
N2	19 (67.9)	6 (75.0)	
Posttreatment N stage			.240
N0	11 (39.3)	1 (12.5)	
N1	11 (39.3)	3 (37.5)	
N2	6 (21.4)	4 (25.0)	
Pretreatment EMVI status			.555
Positive	24 (85.7)	8 (100)	
Negative	4 (14.3)	0	
Posttreatment EMVI status			.422
Positive	11 (39.3)	5 (62.5)	
Negative	17 (60.7)	3 (37.5)	
Intratumoral calcification			.207
Absent	26 (92.9)	6 (75.0)	
Present	2 (7.1)	2 (12.5)	
Tumor necrosis[b]			.397
Absent	20 (71.4)	4 (50.0)	
Present	8 (28.6)	4 (50.0)	
Peritumoral fat infiltration			1.000
Absent	18 (64.3)	5 (67.5)	
Present	10 (35.7)	3 (37.5)	
Intestinal fistula			1.000
Absent	22 (78.6)	6 (75.0)	
Present	6 (21.4)	2 (25.0)	
Vascular sign[c]			.003
Absent	17 (60.7)	0	
Present	11 (39.3)	8 (100)	

TABLE 1 (Continued)

Variable	pCR[a] (n = 28)	Non-pCR (n = 8)	*P*-value
Nodular sign[d]			<.001
Absent	27 (96.4)	1 (12.5)	
Present	1 (4.6)	7 (87.5)	
Extramural enhancement sign[e]			.003
Absent	26 (92.9)	3 (37.5)	
Present	2 (7.1)	5 (62.5)	

Note: Unless otherwise indicated, radiological features were analyzed by posttreatment CT images and data are n (%) unless otherwise indicated.
Abbreviations: CT, computed tomography; EMVI, extramural venous invasion; IQR, interquartile range; pCR, pathological complete response.
[a]Two patients with both a rectum and a colon tumor have pCR.
[b]Tumor necrosis defined as an irregular low attenuation region with the CT attenuation ≤20 HU in each phase and degree of enhancement ≤10 HU within residual lesions in primary tumor site.
[c]Vascular sign defined as striated or punctate vessels remaining within the radiographical residual tumor.
[d]Nodular sign defined as avid enhanced mural nodules in the colorectal canal invaded by the primary tumor.
[e]Extramural enhancement sign defined as extramural area of colorectum with at least mild enhancement.

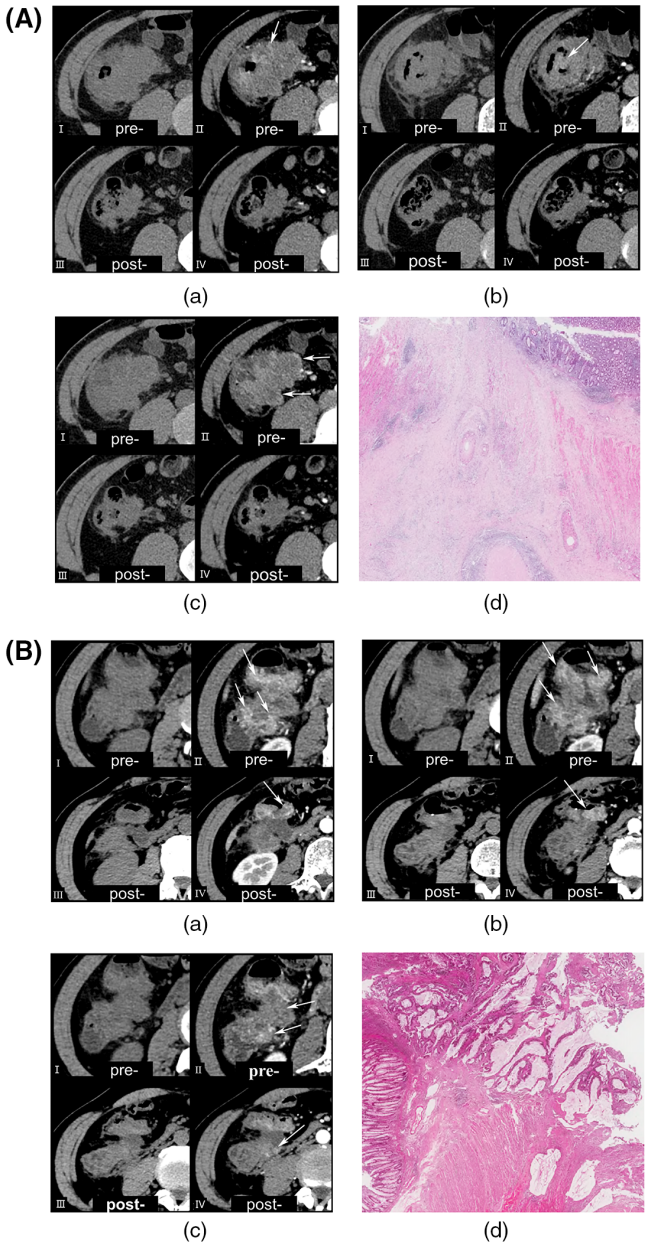

cancers of colon and rectum simultaneously. Of all tumors examined, 28 (77.8%) tumors exhibited pCR, while the remaining 22.2% presented with non-pCR. The characteristics of all primary tumors included in the PICC trial are displayed in Table 1. Both patients with double primary cancers in colon and rectum achieved pCR after PD-1 blockade. Additionally, five (14.7%) patients were suspected to have Lynch syndrome, and 16 (44.4%) tumors exhibited loss of expression of MLH1 or PMS2, or both. Further details are presented in Supporting Information S3.

3.2 | Correlations between CT imaging features and pCR

As shown in Table 1, the posttreatment tumor maximum thickness and the percentage change in tumor maximum thickness from

FIGURE 2 The representative cases of vascular, nodular and extramural enhancement signs. (A) A 36-year-old male with ascending colon cancer. I, III show CT plain scan images pretreatment and posttreatment, respectively, then the II and IV present the corresponding arterial phase of images (a-c). The patient was assessed as absence of vascular, nodular and extramural enhancement signs: (a) no striated or punctate vascular signs within the residual tumor; (b) no avid enhanced mural nodules in the colorectal canal invaded by the primary tumor; (c) the area outside the expected normal intestinal wall without enhancement. The absence of the above signs was predictive for good pathological response. Finally, the patient has proved achieve pathological complete response confirmed by histopathology (d, HE ×40). (B) A 58-year-old male diagnosed with colon cancer of hepatic flexure. I, III show CT plain scan images pretreatment and posttreatment, respectively, then the II and IV present the corresponding arterial phase of images (a-c). The patient was judged as presence of vascular, nodular and extramural enhancement signs: (a) with striated or punctate vascular signs within the residual tumor; (b) with avid enhanced mural nodules in the colorectal canal invaded by the primary tumor; (c) the area outside the expected normal intestinal wall with enhancement. The presence of the above signs was predictive for poor pathological response. Finally, the patient was staged as ypT3N0 by histopathology (d, HE ×40) [Color figure can be viewed at wileyonlinelibrary.com]

baseline presented statistically significant differences between the tumors with pCR and non-pCR. To convert the continuous data into binary data and calculate the OR, we performed ROC curve analysis to determine the optimal classification threshold along with the corresponding Youden index (Supporting Information S4). In detail, the tumors with pCR had smaller posttreatment tumor maximum thickness (median: 10 mm vs 13 mm, $P = .004$), with an OR of 22.440 (95% CI, 1.180-462.764) and higher percentage decrease in tumor maximum thickness from baseline (52.9% vs 21.6%, $P = .005$, OR = 19.519 [95% CI, 1.028-370.716]) compared to non-pCR tumors. No statistically significant differences were observed between tumors with pCR and non-pCR in terms of the percentage change in tumor longitudinal diameter from baseline or TN staging of the primary tumor. Likewise, there was no evidence of a difference in pretreatment EMVI status ($P = .555$), posttreatment EMVI status ($P = .422$), intratumoral calcification ($P = .207$), peritumoral fat infiltration ($P = 1.000$), intestinal fistula ($P = 1.000$) and tumor necrosis ($P = .379$) between the pCR and non-pCR tumors.

3.3 | Relationships between posttherapeutic CT-defined novel features and pCR

The vascular, nodular and extramural enhancement signs showed significant statistical differences between the tumors with pCR and non-pCR (Table 1). Among tumors with pCR, 60.7% (n = 17) presented the absence of vascular sign, and the absence of nodular and extramural enhancement signs was observed in 96.4% and 92.9% of all tumors, respectively. For tumors with non-pCR, the prevalence of the absence of these signs was as follows: vascular sign −0%, nodular sign −12.5% and extramural enhancement sign −37.5%. It is noted that patients with pCR showed a higher tendency to show an absence of vascular sign ($P = .003$, OR = 25.870 [95% CI, 1.357-493.110]), nodular sign ($P < .001$, OR = 189.000 [95% CI, 10.464-3413.803]) and extramural enhancement signs ($P = .003$, OR = 21.667 [95% CI, 2.848-164.830]) than those with non-pCR. Additionally, in terms of tumors with pCR group, we performed a subgroup analysis based on suspected Lynch syndrome and loss of expression of mismatch repair proteins, in order to assess the association of predictive radiological signs (vascular, nodular and extramural enhancement signs, as well as posttreatment tumor maximum thickness and the percentage change in tumormaximum thickness from baseline) with suspected Lynch syndrome and loss of expression of mismatch repair proteins. The results disclosed no statistically significant differences were observed between these subgroups (Supporting Information S3). Figure 2 illustrates the vascular, nodular and extramural enhancement signs of two representative cases together with the corresponding pathological findings.

3.4 | Evaluation agreements on CT imaging features

The distribution of CT imaging features in our study is shown in Figure 3. The details on the interobserver agreements between readers 1 and 2, including the tumor maximum thickness, tumor longitudinal diameter and their corresponding percentage changes from baseline are presented in Supporting Information S1. Additionally, the conformance assessments between readers 1 and 2 in terms of TN staging of the primary tumor, EMVI status, intratumoral calcification, peritumoral fat infiltration, intestinal fistula and tumor necrosis, are described in Supporting Information S5. The kappa values for vascular, nodular and extramural enhancement signs between readers 3 and 4 were found to be high at 0.889, 0.852 and 0.824, respectively. Regarding the repeatability of reader 3, the κ value was 0.944 for the vascular sign, 0.923 for the nodular sign and 0.893 for the extramural enhancement sign.

4 | DISCUSSION

To the best of our knowledge, this is the first study to identify CT-based radiological features associated with pCR after neoadjuvant

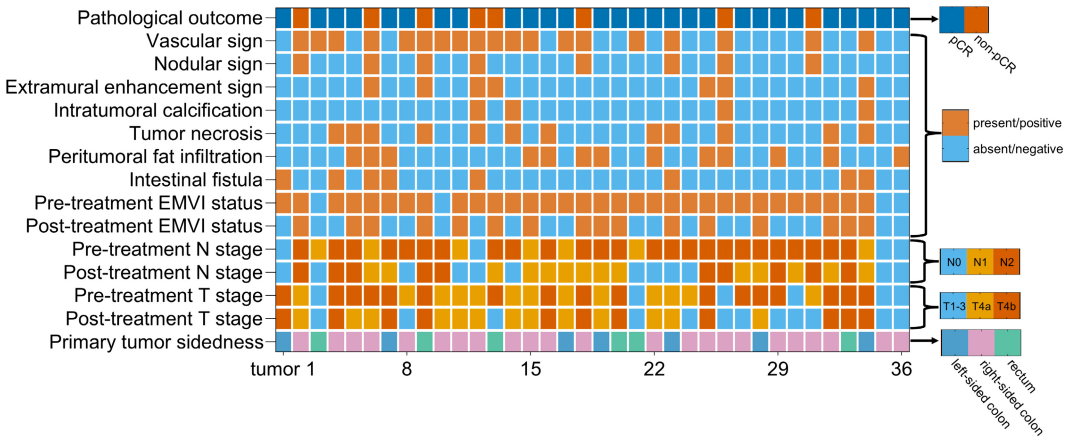

FIGURE 3 Heatmap of CT imaging features in colorectal cancer treated with neoadjuvant PD-1 blockade. Vascular sign defined as striated or punctate vessels remaining within the radiological residual tumor; nodular sign defined as avid enhanced mural nodules in the colorectal canal invaded by the primary tumor; extramural enhancement sign defined as extramural area of colorectum with at least mild enhancement. EMVI, extramural venous invasion; pCR, pathological complete response [Color figure can be viewed at wileyonlinelibrary.com]

PD-1 blockade in dMMR CRC patients based on the PICC phase II trial. Specifically, our results demonstrated that posttreatment tumor maximum thickness and the percentage change in tumor maximum thickness from baseline, as well as the absence of vascular, nodular and extramural enhancement signs were significantly associated with pCR. The identification of these easily identifiable radiological features may have the potential to provide clinicians and radiologists with valuable tools to evaluate the efficacy of neoadjuvant PD-1 blockade in treating dMMR CRC.

Previous scholars have explored some radiological evaluation criteria to identify the therapeutic response, such as the magnetic resonance imaging (MRI) volumetry of diffusion-weighted and T2-weighted sequences, which were raised in patients with locally advanced rectal cancer.[17] It is suggested that the relative proportion of fibrosis within the tumor based on MRI may provide a reference for tumor response evaluation.[18,19] However, postsurgical specimens from patients who achieved pCR after immune checkpoint blockade were characterized by a predominance of acellular mucus pools and necrosis, with fibrosis in the minority.[20] Therefore, these criteria were inapplicable for tumor response evaluation after neoadjuvant PD-1 blockade. Furthermore, it is noteworthy that there are currently no easily accessible CT-based evaluation criteria to identify the actual pathological outcome of the radiological residual lesion after neoadjuvant PD-1 blockade. In this regard, we attempted to excavate pCR-related radiological features to identify patients who may be suitable candidates for a more conservative treatment procedure, such as close monitoring or a watch-and-wait strategy, especially for those individuals presented with radiological residual lesions, that differs significantly from previous researches.

The RECIST (version 1.1) mainly relies on measuring the sum of the longest diameters of the target lesions to evaluate therapeutic response.[11,21,22] Additionally, Fucà et al. discovered that early tumor shrinkage and depth of response were important prognostic factors in microsatellite instability-high metastatic CRC patients treated with immune checkpoint inhibitors.[23] Inspired by their findings, in the present study, we also selected the tumor maximum thickness and tumor longitudinal diameter to assess their associations with therapeutic response after neoadjuvant PD-1 blockade. Differently, the percentage change in tumor longitudinal diameter from baseline was not related to pCR in our study, presenting discrepancies between radiological tumor residual and pathological outcomes after neoadjuvant PD-1 blockade, in line with the findings in the PICC trial.[5] This discordance between histological and radiological findings could be attributed to the infiltration of immune cells, mucus and necrosis changes within the tumor after neoadjuvant PD-1 blockade, which might lead to radiological residual lesions without any activity, as reported in previous literatures.[24,25] However, our results revealed that measurements of tumor thickness have some guidance value for clinicians to identify patients who achieved pCR after neoadjuvant PD-1 blockade. Nevertheless, further validation on larger patient cohorts is necessary to confirm their generalizability and clinical applicability.

In our study, the radiological restaging of the primary tumor after neoadjuvant PD-1 blockade showed a significant discrepancy with the pathological stage. The primary tumors in our enrolled patients were staged as T3-4 at baseline, and an over-restaging of the T stage after treatment was commonly observed, which mainly caused by the radiological residual tumor. After neoadjuvant PD-1 blockade, it should be noted that patients with radiological residual lesion at the primary tumor site may not have viable residual tumor due to changes in necrosis or mucus. Nevertheless, adjacent organs and structures could have been surgically removed owing to misjudgment by radiologists. Therefore, T restaging may not be a reliable indicator to measure the efficacy of neoadjuvant PD-1 blockade in dMMR colorectal cancer.

Generally, the concept of viable tumor has been emphasized and adopted by the expert panel to evaluate the therapeutic efficacy in solid tumors, and complete response refers to the disappearance of any intratumoral arterial enhancement in target lesions, according to modified RECIST guidelines.[26,27] The CT arterial-phase image contains related information of tumor hemodynamics, which is closely associated with tumor activity and could reflect the information of viable residual tumor based on the uptake of contrast agent.[28,29] In our study, we specifically analyzed posttreatment CT arterial-phase images and defined novel radiological features including vascular, nodular and extramural enhancement signs, hypothesizing that these features could potentially be associated with pCR after neoadjuvant PD-1 blockade. To account for interference from the enhancement of intestinal mucosa and muscularity, avid enhancement was considered as the presence of nodular sign. As for extramural enhancement sign without interference from nontumor tissues, at least mild enhancement was defined as present. Assuming the validity of our method, radiologists may potentially utilize easily identifiable vascular, nodular and extramural enhancement signs as effective tools for evaluating tumor response to PD-1 blockade. Notably, such novel radiological features derived from CT images could be incorporated into the clinical workflow without additional burden on patients.

Our study demonstrated the absence of vascular, nodular and extramural enhancement signs on posttreatment CT images was associated with a higher likelihood of achieving pCR in colorectal cancer patients. The findings suggest that patients without these three signs may be suitable candidates for less invasive treatment strategies, rather than extensive surgical intervention. Undoubtedly, it will confer substantial clinical benefits upon patients, particularly for those with radiological residual lesions in pCR cases. Of course, it is acknowledged that the proportion of non-pCR is comparably small in our study, which may introduce bias. Therefore, larger-sample researches are required to validate the effectiveness of the vascular, nodular and extramural enhancement signs in accurately distinguishing non-pCR patients and mitigate the risk of undertreatment in the future. Notably, the 95% CIs of the OR values in our study were wide. We speculate that the possible reason for such a result may be due to the insufficient sample size. We are looking forward to the opportunity to re-examine the value of these radiological signs with a larger sample in the future. It is widely recognized that the resolution of CT imaging is subject to certain limitations, which may be influenced by various factors such as the beam hardening effect, radiation dose, bore size of the CT scanner, as well as respiratory motion. Therefore, there are certain limitations associated with the use

of CT imaging in interpreting some radiological features. As observed in our study, the nodular sign was defined as positive when an avidly enhanced nodule was present, but the degree of enhancement was susceptible to the resolution of CT imaging, which meant that CT scans had limitations in terms of sensitivity and specificity in accurately detecting and characterizing this particular sign. Artificial intelligence-assisted image analysis of CT parameters may hold the potential to address these challenges in the future. At all events, the proposal of an easy-to-use radiological feature may furnish clinicians with a reference for accurately identifying pCR prior to surgery, and advancing precision medicine.

Our study has its own limitations. First, it was a post hoc study conducted on a relatively small sample size from a single-center, derived from a prospective cohort of the PICC phase II trial. Moreover, to achieve better clinical application, rigorous testing and validation of the proposed radiological features in larger databases from multiple centers are necessary. Second, the relationship between CT-defined features and prognosis is unknown because of the short post-operative follow-up period. To date, no adverse events including death, local recurrence or distant metastase have been observed in these colorectal cancer patients. Third, our study lacks information on the prevalence of MLH1 methylation or BRAF mutations in MLH1-negative tumors due to the limited analysis conducted on biopsied samples. The biopsied samples obtained prior to neoadjuvant immunotherapy were analyzed first for MMR or MSI status using immunohistochemistry or polymerase chain reaction (PCR). Consequently, these samples were insufficient for further other analysis. The postoperative specimens, although obtained after surgical removal of the lesions, were inadequate for exploring BRAF mutations and MLH1 promoter methylation status, as the 97% of them achieved a major pathological response. Additionally, although we initially screened patients suspected of having Lynch syndrome using the Amsterdam II criteria, we did not conduct further testing for germline mutations to confirm the presence of Lynch syndrome. In our study, over 50% of the patients had MSH2/MSH6-negative tumors. These patients had a higher likelihood of having Lynch syndrome compared to those with MLH1/PMS2-negative tumors, even if they did not meet the Amsterdam II criteria. Furthermore, our study specifically examined radiological features based on routine CT images, as opposed to other imaging technologies. However, CT remains the widely used examination method for CRC, particularly in colon cancer, due to its ability to overcome limitations related to abdominal gas and intestinal bowel motion artifacts that can affect the application of MRI. Additionally, these CT imaging features can be seamlessly integrated into the clinical workflow without imposing any additional burden on patients. We anticipate that other new imaging techniques will be conducive to evaluating tumor therapeutic response in the future.

5 | CONCLUSION

In summary, we conducted a preliminary exploration of radiological features based on CT images after neoadjuvant PD-1 blockade in dMMR CRC, and found that posttreatment tumor maximum thickness, the percentage change in tumor maximum thickness from baseline, as well as the absence of vascular, nodular and extramural enhancement signs were significantly associated with pCR. These CT-defined radiological features may have the potential to serve as valuable tools for clinicians in identifying patients who have achieved pCR after neoadjuvant PD-1 blockade, particularly in individuals who are willing to adopt a watch-and-wait strategy.

AUTHOR CONTRIBUTIONS

Wuteng Cao, Huabin Hu and Yanhong Deng conceived and designed the study; Wuteng Cao, Huabin Hu and Qianyu Wu collected and assembled data, Wuteng Cao, Jiao Li, Qianyu Wu, Biao Li, Jie Zhou, Xinhua Wang analyzed the medical images; Wuteng Cao, Lishuo Shi and Junhong Chen performed statistical analysis; Chao Wang, Huaiming Wang, Weihao Deng and Yan Huang analyzed the resected pathological specimens; Wuteng Cao, Huabin Hu and Yanhong Deng wrote the paper. All authors read and approved the final manuscript. The work reported in the paper has been performed by the authors unless clearly specified in the text.

ACKNOWLEDGEMENTS

Our research was supported by the National Key Clinical Discipline, the program of Guangdong Provincial Clinical Research Center for Digestive Diseases (2020B1111170004) and the Chinese Society of Clinical Oncology-JunshiBiosciences Oncology Immunity Research Fund (Y-JS2019-055). We thank Pan Luo and Ting Sun for assistance in the schematic processing. We also thank Wenhao Zhu for medical writing assistance and used ChatGPT for English language editing.

FUNDING INFORMATION

Our study was supported by the National Natural Science Foundation of China (82001765, 82272800).

CONFLICT OF INTEREST STATEMENT

The authors declare that they have no conflict of interests.

DATA AVAILABILITY STATEMENT

The data that support the findings of our study are available from the corresponding author upon reasonable request.

ETHICS STATEMENT

The study protocol was approved by the Medical Ethics Committee of the Sixth Affiliated Hospital, Sun Yat-sen University and written informed consent was waived due to the retrospective study.

ORCID

Wuteng Cao https://orcid.org/0000-0001-5854-6012
Huabin Hu https://orcid.org/0000-0001-6539-9401
Jiao Li https://orcid.org/0000-0002-6322-586X
Qianyu Wu https://orcid.org/0009-0003-7008-4844
Lishuo Shi https://orcid.org/0000-0002-0715-9941
Biao Li https://orcid.org/0009-0009-5707-5314

Jie Zhou https://orcid.org/0000-0002-0960-0665
Xinhua Wang https://orcid.org/0009-0002-6644-0562
Junhong Chen https://orcid.org/0000-0002-8313-8317
Chao Wang https://orcid.org/0000-0001-5453-3927
Huaiming Wang https://orcid.org/0000-0003-3126-4618
Weihao Deng https://orcid.org/0009-0001-2287-0061
Yan Huang https://orcid.org/0000-0003-4822-5615
Yanhong Deng https://orcid.org/0000-0001-6873-8026

REFERENCES

1. Emens LA. Breast cancer immunotherapy: facts and hopes. *Clin Cancer Res*. 2018;24:511-520.
2. Lote H, Cafferkey C, Chau I. PD-1 and PD-L1 blockade in gastrointestinal malignancies. *Cancer Treat Rev*. 2015;41:893-903.
3. Le DT, Kim TW, Van Cutsem E, et al. Phase II open-label study of pembrolizumab in treatment-refractory, microsatellite instability-high/mismatch repair-deficient metastatic colorectal cancer: KEYNOTE-164. *J Clin Oncol*. 2020;38:11-19.
4. Chalabi M, Fanchi LF, Dijkstra KK, et al. Neoadjuvant immunotherapy leads to pathological responses in MMR-proficient and MMR-deficient early-stage colon cancers. *Nat Med*. 2020;26:566-576.
5. Hu H, Kang L, Zhang J, et al. Neoadjuvant PD-1 blockade with toripalimab, with or without celecoxib, in mismatch repair-deficient or microsatellite instability-high, locally advanced, colorectal cancer (PICC): a single-centre, parallel-group, non-comparative, randomised, phase 2 trial. *Lancet Gastroenterol Hepatol*. 2022;7:38-48.
6. Cercek A, Lumish M. PD-1 blockade in mismatch repair-deficient, locally advanced rectal cancer. *N Engl J Med*. 2022;386:2363-2376.
7. Maas M, Beets-Tan RGH, Lambregts DMJ, et al. Wait-and-see policy for clinical complete responders after chemoradiation for rectal cancer. *J Clin Oncol*. 2011;29:4633-4640.
8. Petrelli F, Trevisan F, Cabiddu M, et al. Total neoadjuvant therapy in rectal cancer: a systematic review and meta-analysis of treatment outcomes. *Ann Surg*. 2020;271:440-448.
9. Hoos A, Wolchok JD, Humphrey RW, Hodi FS. CCR20th anniversary commentary: immune-related response criteria—capturing clinical activity in immuno-oncology. *Clin Cancer Res*. 2015;21:4989-4991.
10. Schadendorf D, Hodi FS, Robert C, et al. Pooled analysis of long-term survival data from phase II and phase III trials of ipilimumab in unresectable or metastatic melanoma. *J Clin Oncol*. 2015;33:1889-1894.
11. Eisenhauer EA, Therasse P, Bogaerts J, et al. New response evaluation criteria in solid tumours: revised RECIST guideline (version 1.1). *Eur J Cancer*. 2009;45:228-247.
12. Zhang C, Pu K. Molecular and nanoengineering approaches towards activatable cancer immunotherapy. *Chem Soc Rev*. 2020;49:4234-4253.
13. Hellmann MD, Chaft JE, William WN Jr, et al. Pathological response after neoadjuvant chemotherapy in resectable non-small-cell lung cancers: proposal for the use of major pathological response as a surrogate endpoint. *Lancet Oncol*. 2014;15:e42-e50.
14. Kaltsas G, Rockall A, Papadogias D, Reznek R, Grossman AB. Recent advances in radiological and radionuclide imaging and therapy of neuroendocrine tumours. *Eur J Endocrinol*. 2004;151:15-27.
15. Wang D, Zhang GB, Yan L, Wei XE, Zhang YZ, Li WB. CT and enhanced CT in diagnosis of gastrointestinal neuroendocrine carcinomas. *Abdom Imaging*. 2012;37:738-745.
16. Amin MB, Greene FL, Edge SB, et al. The eighth edition AJCC cancer staging manual: continuing to build a bridge from a population-based to a more "personalized" approach to cancer staging. *CA Cancer J Clin*. 2017;67:93-99.
17. Curvo-Semedo L, Lambregts DM, Maas M, et al. Rectal cancer: assessment of complete response to preoperative combined radiation therapy with chemotherapy—conventional MR Volumetry versus diffusion-weighted MR imaging. *Radiology*. 2011;260:734-743.
18. Patel UB, Brown G, Machado I, et al. MRI assessment and outcomes in patients receiving neoadjuvant chemotherapy only for primary rectal cancer: long-term results from the GEMCAD 0801 trial. *Ann Oncol*. 2017;28:344-353.
19. Patel UB, Taylor F, Blomqvist L, et al. Magnetic resonance imaging-detected tumor response for locally advanced rectal cancer predicts survival outcomes: MERCURY experience. *J Clin Oncol*. 2011;29:3753-3760.
20. Ludford K, Cohen R, Svrcek M, et al. Pathological tumor response following immune checkpoint blockade for deficient mismatch repair advanced colorectal cancer. *J Natl Cancer Inst*. 2021;113:208-211.
21. Dancey JE, Dodd LE, Ford R, et al. Recommendations for the assessment of progression in randomised cancer treatment trials. *Eur J Cancer*. 2009;45:281-289.
22. Therasse P, Arbuck SG, Eisenhauer EA, et al. New guidelines to evaluate the response to treatment in solid tumors. European Organization for Research and Treatment of cancer, National Cancer Institute of the United States, National Cancer Institute of Canada. *J Natl Cancer Inst*. 2000;92:205-216.
23. Fuca G, Corti F, Ambrosini M, et al. Prognostic impact of early tumor shrinkage and depth of response in patients with microsatellite instability-high metastatic colorectal cancer receiving immune checkpoint inhibitors. *J Immunother Cancer*. 2021;9:9.
24. Amaria RN, Reddy SM, Tawbi HA, et al. Neoadjuvant immune checkpoint blockade in high-risk resectable melanoma. *Nat Med*. 2018;24:1649-1654.
25. Forde PM, Chaft JE, Smith KN, Anagnostou V, Cottrell TR, Hellmann MD. Neoadjuvant PD-1 blockade in resectable. *Lung Cancer*. 2018;378:1976-1986.
26. Bruix J, Sherman M. Practice guidelines committee AAftSoLD. *Manag Hepatocell Carcinoma Hepatol*. 2005;42:1208-1236.
27. Gillmore R, Stuart S, Kirkwood A, et al. EASL and mRECIST responses are independent prognostic factors for survival in hepatocellular cancer patients treated with transarterial embolization. *J Hepatol*. 2011;55:1309-1316.
28. van Persijn van Meerten EL, Gelderblom H, Bloem JL. RECIST revised: implications for the radiologist—a review article on the modified RECIST guideline. *Eur Radiol*. 2010;20:1456-1467.
29. Llovet JM, Lencioni R. mRECIST for HCC: performance and novel refinements. *J Hepatol*. 2020;72:288-306.

SUPPORTING INFORMATION

Additional supporting information can be found online in the Supporting Information section at the end of this article.

How to cite this article: Cao W, Hu H, Li J, et al. China special issue on gastrointestinal tumors-Radiological features of pathological complete response in mismatch repair deficient colorectal cancer after neoadjuvant PD-1 blockade: A post hoc analysis of the PICC phase II trial. *Int J Cancer*. 2023;153(11):1894-1903. doi:10.1002/ijc.34647